A threading receptor for polysaccharides

Tiddo J. Mooibroek[1], **Juan M. Casas-Solvas**[1,2], **Robert L. Harniman**[1], **Charles M. Renney**[1], **Tom S. Carter**[1], **Matthew P. Crump**[1], and **Anthony P. Davis**[1,*]

[1]School of Chemistry, University of Bristol, Cantock's Close, Bristol, BS8 1TS, UK

[2]Department of Chemistry and Physics, University of Almería, Carretera de Sacramento s/n, 04120 Almería, Spain

Abstract

Cellulose, chitin and related polysaccharides are key renewable sources of organic molecules and materials. However, poor solubility tends to hamper their exploitation. Synthetic receptors could aid dissolution provided they are capable of cooperative action, for example by multiple threading on a single polysaccharide molecule. Here we report a synthetic receptor designed to form threaded complexes (polypseudorotaxanes) with these natural polymers. The receptor binds fragments of the polysaccharides in aqueous solution with high affinities (K_a up to 19,000 M^{-1}), and is shown to adopt the threading geometry by nuclear Overhauser effect spectroscopy (NOESY). Evidence from induced circular dichroism (ICD) and atomic force microscopy (AFM) implies that the receptor also forms polypseudorotaxanes with cellulose and its polycationic analogue chitosan. The results hold promise for polysaccharide solubilisation under mild conditions, as well as new approaches to biological activity.

Polysaccharides are the dominant organic molecules in the biosphere1, and thus key renewable resources2,3. However the most abundant, including cellulose and chitin, are generally the most difficult to utilise due to extreme insolubility. At present there is no method for mobilising these materials in water under mild conditions, so that modifications involve chemical transformations in aggressive media4–6 or the slow action of enzymes on undissolved solids7. Dissolution in aqueous media at biological pH would allow new paths to exploitation. In particular, the polysaccharides could be exposed to enzymes, either natural or engineered, to which they would be far more vulnerable. The rapid conversion of cellulose to glucose is just one prospective outcome.

Here we adumbrate a strategy for the dissolution of cellulose, and related polysaccharides, through the application of synthetic receptors. The approach employs cage molecules with amphiphilic interiors, complementary to the carbohydrate targets. Critically the receptors are able to thread onto the polysaccharides, forming polypseudorotaxanes[8,9]. Because of the threaded topology, many receptor molecules can bind to one polysaccharide chain, surrounding the polymer with hydrophilic groups. If binding is sufficiently strong to counteract crystal packing forces, dissolution should be feasible. We report the design and synthesis of a threading receptor for polysaccharides, and show that it forms pseudorotaxanes with water-soluble oligosaccharides. We also describe evidence for polypseudorotaxane formation from polysaccharides under certain conditions. The results demonstrate the feasibility of polysaccharide threading in water, and could point the way to systems capable of solubilisation.

A defining feature of cellulose **1** and chitin **2** (Fig. 1a) is the all-equatorial disposition of intra-chain linkages and polar substituents and (consequently) the axial positioning of apolar CH groups. In the extended conformation of the polymer, this creates two parallel strips of hydrophobic surface separated by lines of hydrogen-bonding functional groups. Our strategy for complementing these supramolecular valencies is illustrated in Fig. 1b. We sought a cage-like receptor structure in which two aromatic surfaces would be held parallel to each other, separated by rigid, polar spacers. The portals of the cage would be large enough to allow threading by the polysaccharide substrates. The aromatic surfaces would be capable of forming hydrophobic and CH-π interactions with axial CH groups in the substrates, while polar groups would hydrogen bond to equatorial substituents.

We had previously used a related approach to bind all-equatorial mono- and di-saccharides in water[10–13]. However, these earlier designs employed flexible biphenyl[10,11] or terphenyl[12,13] units as aromatic surfaces, and required four or five spacers to maintain preorganised cavities. The resulting cage structures were successful but size-specific; they encapsulated their targets, did not allow threading, and could not be applied to polysaccharides. The challenge here was to create a maintained cavity using fewer spacers and a more open architecture. Our proposed solution was to exploit condensed aromatic units as extended, rigid hydrophobic surfaces. Specifically, the tetracyclic pyrene possesses a surface which easily spans a monosaccharide residue. Two pyrene units and three isophthalamide spacers may be combined to form the symmetrical bicyclic structure **4** (Fig. 1c). Molecular modelling predicted that **4** would retain an open structure in water, despite the potential for hydrophobically-driven collapse, and that a cellulose chain could indeed pass through the larger portals of the cavity while hydrogen bonding to annular amides in the spacers (cf. Fig. 1b, see also Fig. 2c). The design also incorporates three externally-directed dendrimeric nonacarboxylate units to ensure water-solubility[14,15].

Results and Discussion

Receptor **4** was synthesized from pyrene via pyrene-2-carboxylic acid[16] as described in Supplementary Section 1. Solutions of **4** in water at pH = 7 and 25 °C gave moderately-resolved ^{1}H nuclear magnetic resonance (NMR) spectra which did not change significantly between 1 mM and 5 μM, implying that the receptor was monomeric over this range of

concentrations (see Supplementary Fig. 2). On warming to 80 °C the resolution improved, consistent with conformational mobility which is fast at the higher temperature but slow enough to cause signal broadening at 25 °C (see Supplementary Fig. 3). Possible motions are rotations of the annular amide groups between "NH-in" orientations as shown in Fig. 1, and "NH-out" where the amide carbonyl points inwards. Evidence for such movements was provided by NOESY connections between the amide protons and spacer aromatic CH groups. For example, integration of NOESY cross-peaks between s3'NH and inward-directed s4', as against outward-directed s2', implied that this NH is 87% "NH-in" and 13% "NH-out" at 25 °C. The equilibrium position was found to be temperature-dependent, the "NH-in" conformation predominating by 81% and 93% at 5 °C and 80 °C respectively (see Supplementary Figs. 4-7).

The binding properties of **4** were studied using ^{1}H NMR titrations and isothermal titration calorimetry (ITC) in aqueous solution. Details are given in Supplementary Section 2. The monosaccharides **5**-**9** and a series of all-equatorial oligosaccharides (see Table 1) were used as substrates. In most cases, addition of carbohydrate to **4** caused movements of receptor ^{1}H NMR signals, consistent with complex formation which is fast on the NMR timescale. The changes are illustrated in Fig. 2a for **4** + cellobiose; these spectra were acquired at 80 °C to reduce signal broadening, but similar movements could be observed and followed at 25 °C. The splitting of some receptor signals (e.g. S2') is consistent with a C_{2v} receptor such as **4** in fast exchange with an asymmetrical substrate (for clarification, see Supplementary Fig. 8). For the monosaccharides, and also for chitobiose (**3**, n = 1), affinities could be quantified by nonlinear least-squares curve fitting of the NMR signal movements assuming a 1:1 binding model. Supporting values for methyl glucoside (**8**) and GlcNAc-β OMe (**9**) could be obtained from ITC. For the cellodextrins **1** the NMR plots showed signs that further substrate molecules could bind weakly to the initial 1:1 complex (see Supplementary Figs. 14 and 15). However, ITC gave plots which fit well to a 1:1 binding model (see Fig. 3 and Supplementary Figs. 17-23). As weak secondary binding is unlikely to interfere with ITC analysis (due to the small thermal signal) the derived association constants were considered reliable. ITC was also employed for chitodextrins **2** (see Supplementary Figs. 24 and 25), as NMR titrations gave signal broadening. The results from both NMR and ITC are summarized in Table 1. Where both methods could be used they showed good agreement.

The results in Table 1 show that, as expected, receptor **4** is selective for all-equatorial carbohydrates, favouring glucose (**7**) and glucoside (**8**) over mannose (**5**) or galactose (**6**). While the binding constants for **7**, **8** and cellobiose are slightly higher than the best previously reported from our laboratory[17,11], the performance with the higher cellodextrins is outstanding. In contrast to earlier systems which showed almost no affinity for these substrates[9,11], receptor **4** binds **1** (n = 2-5) with Ka = 5,000 M^{-1} or greater. The binding constant for cellotetraose, at ˜12,000 M^{-1}, is the highest observed for biomimetic recognition of a neutral saccharide in water. While the affinities seem to peak at cellotetraose, there is no sign of an upper limit for length of substrate. It is interesting to note that variations within the cellodextrin series are determined more by entropy than enthalpy. It is understandable that the enthalpies for **1** (n = 1-5) should be roughly similar, as the interactions made and broken during binding should be nearly the same. It is also reasonable

that the entropy of binding should become more favourable in the series cellobiose → cellotriose → cellotetraose (**1**, n = 1-3). As the substrate becomes longer it gains freedom of movement in the complex, thus gaining translational entropy. It is less obvious why the entropy of binding should peak at cellotetraose (**1**, n = 3), but this might relate to contacts between substrate and side-chains, which could restrict the motion of both. This is consistent with modelling. For complexes with cellobiose-cellotetraose the receptor side chains appear largely unconstrained. However for cellopentaose and longer substrates, the polysaccharide chain begins to clash with the side-chains at the more crowded, "double-spacer" end of the receptor.

The binding constant to cationic chitobiose (**3**, n = 1) is even higher than that for cellotetraose, though this is unsurprising considering the charge complementarity between receptor and substrate. Acetylated chitodextrins **2** (n = 1,2) were bound less strongly but still substantially. Although the affinities to **4** might seem moderate by general biological standards, it should be noted that carbohydrates in water are challenging targets[18]. The values measured are well within the range observed for lectins, the major class of carbohydrate-binding proteins[19].

To confirm that **4** could thread fully onto oligosaccharides, rather than staying at one end, we performed a NOESY-based structural investigation on the complex between **4** and cellopentaose (**1**, n = 4). In the ^{1}H NMR spectrum of cellopentaose, it is possible to differentiate between internal residues II-IV and terminal residues I and V (see Fig. 2b)[20,21]. In the NOESY spectrum of **4**·cellopentaose, strong cross-peaks were observed from pyrenyl protons p4/p5 to internal residues II-IV, very weak signals to the non-reducing terminus V, and none to reducing terminus I (Fig. 2b). Even allowing for the three-fold near-degeneracy of the internal residue signals, the results imply that the receptor spends most of its time in the middle of the pentasaccharide (Fig. 2c). Spectra of **4** with cellobiose and cellotriose supported this interpretation (see Supplementary Fig. 34).

Having confirmed the threading geometry for oligosaccharide binding, we investigated whether **4** could form polypseudorotaxanes with all-equatorial polysaccharides. To study cellulose + **4** we dissolved the polysaccharide and receptor in 1 M NaOH[22]. Previous experiments had shown that the receptor is stable to strong aqueous base (which was used in the final deprotection step in the synthesis). Induced circular dichroism (ICD) was observed across the absorbance range of the pyrene units in the receptor (see Supplementary Fig. 36) implying close contact between the cellulose (which may be partially deprotonated) and some molecules of receptor[11,12]. Given the NMR evidence for cellodextrin threading, and the literature precedent for polypseudorotaxanes[9], it seems reasonable to infer the formation of multiply threaded complexes. Dilution of such solutions with water by 2.5×10^5, followed by deposition on mica and washing with water, gave samples suitable for study by AFM. A resulting image is shown in Fig. 4a. The principle large scale feature is a long strand which is ˜1 nm broad in some regions and ˜2 nm in others. This is consistent with cellulose molecules pairing and overlapping over part of their lengths. Along the feature (in particular along the narrower parts), higher and wider bulb-like protrusions are present. The average dimensions of 34 of these protrusions were determined as 1.14 ± 0.17 nm high and 2.9 ± 0.90 nm wide. Both are consistent with the dimensions estimated for individual

receptor molecules (see Supplementary Fig. 37), and the image thus seems to indicate the threading of multiple receptors onto the cellulose. The alternative arrangement in which receptor molecules lie on top of the cellulose should give protrusions   1.6 nm in height. The population of threaded receptors cannot be related to an equilibrium in solution, because the sample underwent major changes in conditions (high concentration/pH, dilution, then returning to high concentrations on evaporation). Moreover the experiment does not show that receptor **4** itself can solubilise cellulose at moderate pH. However, it does seem to provide the first evidence of a polysaccharide-based polypseudorotaxane architecture. Control samples prepared from cellulose alone showed compact features which appeared to consist of multiple intertwined cellulose molecules (see Fig. 4b). This suggests that, unsurprisingly, polypseudorotaxane formation affects cellulose folding and promotes extended rather than coiled conformations. Further details and discussion of the AFM measurements are presented in Supplementary Section 5.

Studies were also performed with chitosan **3** (n = 375-750) which is soluble under mildly acidic conditions (pH ≈ 6). Mixtures of chitosan and **4** were found to give clear solutions across the pH range 1-11. As chitosan is insoluble at basic pH, and receptor **4** is insoluble in acid, this implied mutual solubilisation. Moreover, the interaction would not seem to depend on electrostatic forces, as one component should be electrically neutral at either end of the range. It thus seems that the solubilisation is not the result of chitosan binding to the receptor side-chains, but to some other interaction geometry, most obviously threading to form polypseudorotaxanes. In support of this interpretation, several ICD bands were observed for chitosan + **4** at pH = 6.4, (see Supplementary Fig. 36). The chitosan + **4** mixture was further studied by AFM. A solution of chitosan + **4** at pH = 1 was diluted with water by 2.5×10^7 then deposited on mica. AFM imaging revealed elongated plate-like structures, as illustrated in Fig. 5a and Supplementary Fig. 37. Height profiles taken along the short axis of the structures gave an average value of ˜1.3 nm, with variations suggesting underlying periodicity (3.5 – 3.8 nm lateral repeat unit, see Fig. 5b). The data are consistent with bundles of aligned polypseudorotaxanes, one unit thick, cemented by hydrogen bonding between receptor carboxyl groups. A computational model of this arrangement (see Fig. 5a) featured inter-chain distances of ˜3.6 nm, consistent with the AFM data. Although the chitosan cannot be detected directly in the image, its presence can be inferred from the organisation imposed on the assemblies. Also, the lengths of the aggregates, at ˜200-500 nm, are consistent with the estimated length range of the chitosan (188 – 375 nm). Control samples prepared from chitosan alone showed mainly coiled structures (see Fig. 5c and Supplementary Fig. 42) while receptor **4** alone, deposited from acid, gave irregular particles with widely varying sizes (see for example Fig. 5d). As argued for **4** + cellulose, the alternative arrangement in which receptor stacks on chitosan should result in measured heights of   1.6 nm, and is therefore inconsistent with the AFM data. For further details and discussion of the AFM measurements, see Supplementary Section 5. The formation of multistrand polypseudorotaxane assemblies with closely-packed macrocycles finds precedent in the well-known complexes of poly(ethylene glycol)s with α-cyclodextrin9.

Conclusion

In conclusion, we have shown that receptor **4** can form threaded complexes with oligo/polysaccharides, with affinities rising above $10^4\,M^{-1}$. The solubilisation of cellulose or chitin through polypseudorotaxane formation will probably require yet stronger binding, to overcome the forces between polysaccharide chains. However, this should be achievable by expanding the hydrophobic surfaces and supplementing the polar interactions. Meanwhile soluble polysaccharides such as chitosan are already important for tissue engineering[23,24], and their applications may multiply in future. Polypseudorotaxane formation could provide a novel means of moderating their properties. Also, the biological importance of cellulose, chitin etc. suggests new modes of biological activity. For example, chitin is a major component of fungal cell walls, and a target for plant defence proteins[25]. Threading onto nascent chitin chains could provide a promising approach to antifungal agents. Finally, while threaded molecular architectures have attracted intense interest in recent years[26,27], we believe these are the first to be formed from a synthetic receptor with biopolymers under biological (i.e. aqueous) conditions. They are therefore the first with potential for direct exploitation in biochemistry or chemical biology.

Supplementary Material

Refer to Web version on PubMed Central for supplementary material.

Acknowledgments

References

1. Voet, D., Voet, JG. Biochemistry. Wiley; New York: 1995.

2. Klemm D, et al. Nanocelluloses: A new family of nature-based materials. Angew Chem Int Ed. 2011; 50:5438–5466.

3. Klemm D, Heublein B, Fink HP, Bohn A. Cellulose: Fascinating biopolymer and sustainable raw material. Angew Chem Int Ed. 2005; 44:3358–3393.

4. Heinze T, Liebert T. Unconventional methods in cellulose functionalization. Prog Polym Sci. 2001; 26:1689–1762.

5. Zhou CH, Xia X, Lin CX, Tong DS, Beltramini J. Catalytic conversion of lignocellulosic biomass to fine chemicals and fuels. Chem Soc Rev. 2011; 40:5588–5617. [PubMed: 21863197]

6. Pinkert A, Marsh KN, Pang SS, Staiger MP. Ionic liquids and their interaction with cellulose. Chem Rev. 2009; 109:6712–6728. [PubMed: 19757807]

7. Brunecky R, et al. Revealing nature's cellulase diversity: The digestion mechanism of Caldicellulosiruptor bescii CelA. Science. 2013; 342:1513–1516. [PubMed: 24357319]

8. Raymo FM, Stoddart JF. Interlocked macromolecules. Chem Rev. 1999; 99:1643–1663. [PubMed: 11849006]

9. Harada A, Hashidzume A, Yamaguchi H, Takashima Y. Polymeric rotaxanes. Chem Rev. 2009; 109:5974–6023. [PubMed: 19736930]

10. Barwell NP, Crump MP, Davis AP. A synthetic lectin for beta-glucosyl. Angew Chem Int Ed. 2009; 48:7673–7676.

11. Ferrand Y, et al. A synthetic lectin for O-linked beta-N-acetylglucosamine. Angew Chem Int Ed. 2009; 48:1775–1779.

12. Ferrand Y, Crump MP, Davis AP. A synthetic lectin analog for biomimetic disaccharide recognition. Science. 2007; 318:619–622. [PubMed: 17962557]

13. Sookcharoenpinyo B, et al. High-affinity disaccharide binding by tricyclic synthetic lectins. Angew Chem Int Ed. 2012; 51:4586–4590.

14. Newkome GR, Shreiner C. Dendrimers derived from $1 \rightarrow 3$ branching motifs. Chem Rev. 2010; 110:6338–6442. [PubMed: 20666373]

15. Diederich F, Felber B. Supramolecular chemistry of dendrimers with functional cores. Proc Natl Acad Sci USA. 2002; 99:4778–4781. [PubMed: 11891306]

16. Casas-Solvas JM, Mooibroek TJ, Sandramurthy S, Howgego JD, Davis AP. A practical, large-scale synthesis of pyrene-2-carboxylic acid. Synlett. 2014; 25:2591–2594.

17. Destecroix H, et al. Affinity enhancements by dendritic side-chains in synthetic carbohydrate receptors. Angew Chem Int Ed. 2015; 54:2057–2061.

18. Ambrosi M, Cameron NR, Davis BG. Lectins: tools for the molecular understanding of the glycocode. Org Biomol Chem. 2005; 3:1593–1608. [PubMed: 15858635]

19. Toone EJ. Structure and energetics of protein-carbohydrate complexes. Curr Opin Struct Biol. 1994; 4:719–728.

20. Flugge LA, Blank JT, Petillo PA. Isolation, modification, and NMR assignments of a series of cellulose oligomers. J Am Chem Soc. 1999; 121:7228–7238.

21. Roslund MU, Tahtinen P, Niemitz M, Sjoholm R. Complete assignments of the H-1 and C-13 chemical shifts and J(H,H) coupling constants in NMR spectra of D-glucopyranose and all D-glucopyranosyl-D-glucopyranosides. Carbohydr Res. 2008; 343:101–112. [PubMed: 17980865]

22. Isogai A, Atalla RH. Dissolution of cellulose in aqueous NaOH solutions. Cellulose. 1998; 5:309–319.

23. Kumar M, Muzzarelli RAA, Muzzarelli C, Sashiwa H, Domb AJ. Chitosan chemistry and pharmaceutical perspectives. Chem Rev. 2004; 104:6017–6084. [PubMed: 15584695]

24. Kharkar PM, Kiick KL, Kloxin AM. Designing degradable hydrogels for orthogonal control of cell microenvironments. Chem Soc Rev. 2013; 42:7335–7372. [PubMed: 23609001]

25. Theis T, Stahl U. Antifungal proteins: targets, mechanisms and prospective applications. Cell Mol Life Sci. 2004; 61:437–455. [PubMed: 14999404]

26. Balzani V, Credi A, Raymo FM, Stoddart JF. Artificial molecular machines. Angew Chem Int Ed. 2000; 39:3349–3391.

27. Kay ER, Leigh DA, Zerbetto F. Synthetic molecular motors and mechanical machines. Angew Chem Int Ed. 2007; 46:72–191.
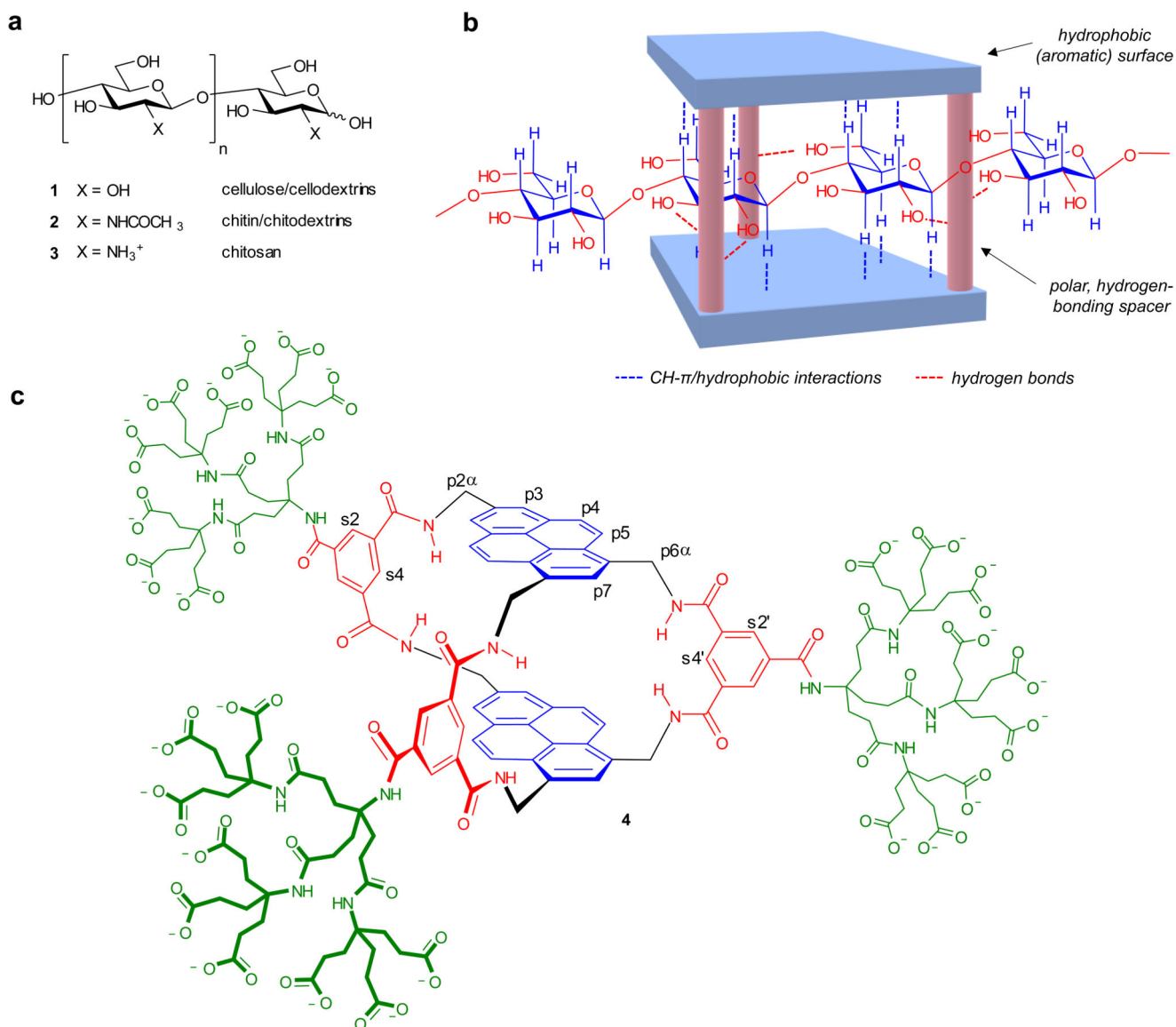
Fig. 1. Receptor design.

a, All-equatorial oligo- and polysaccharide targets. **b**, Schematic design strategy, with cellulose depicted as substrate. **c**, Polysaccharide receptor **4**, with labels for selected carbons. The complete labelling system is given in Supplementary Figure 1. For **b** and **c**, the hydrophobic and polar moieties in the receptor core are shown in blue and red respectively.
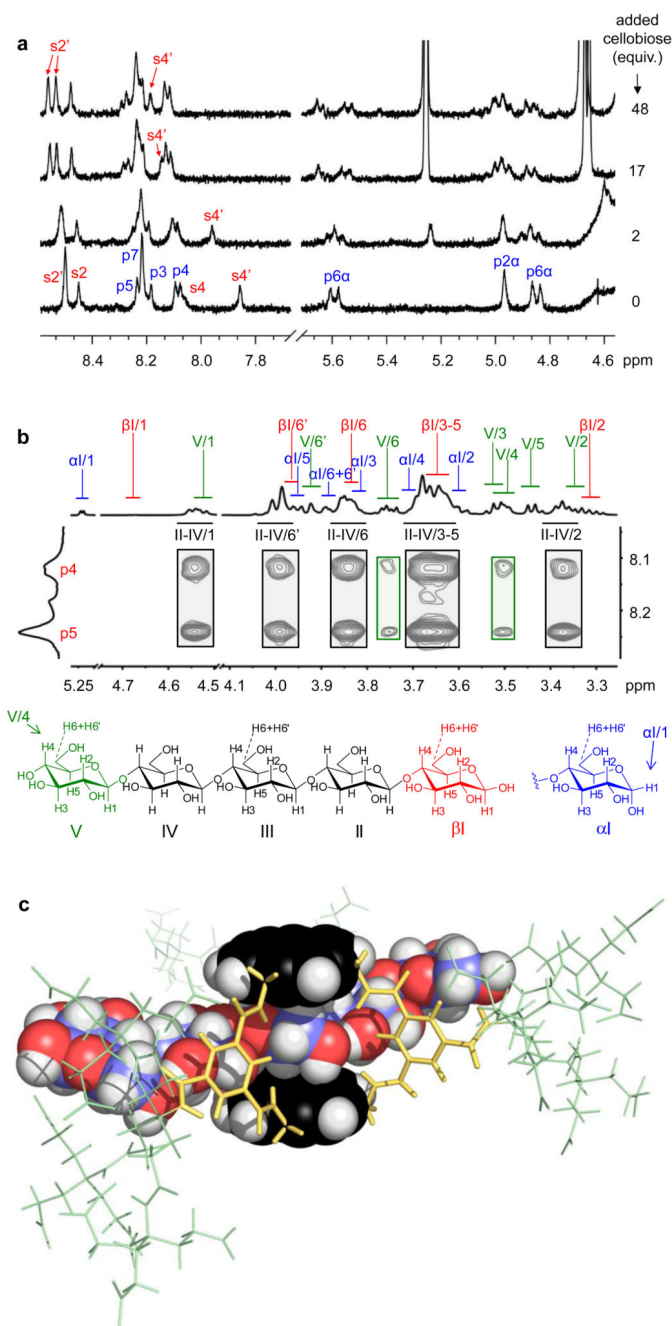
Fig. 2. ^{1}H NMR evidence for receptor 4 binding oligosaccharides.
a, Partial spectra (500 MHz) from a titration of **4** (0.5 mM) against D-cellobiose (**1**, n = 1) in D₂O at 80 °C. See Fig. 1 for proton numbering. **b,** Partial NOESY spectrum (D₂O, 600 MHz) of **4** (0.25 mM) + D-cellopentaose **1** (n = 4) (4.7 mM), with assignments. Cross-peaks to internal saccharide residues II-IV (black rectangles) dominate the spectrum. **c,** Calculated structure of **4** + **1** (n = 4) consistent with the NOESY spectrum. The pyrene units and cellopentaose are shown in spacefilling mode: yellow, isophthalamide spacers; green, side-chains; black, pyrenyl carbon; blue, carbohydrate carbon; red, oxygen; white, hydrogen. The

conformation was energy-minimised using MacroModel 10.3 (Maestro 9.7 interface) with the Merck Molecular Force Field (static) and Generalized Born/Surface Area (water) continuum solvation.
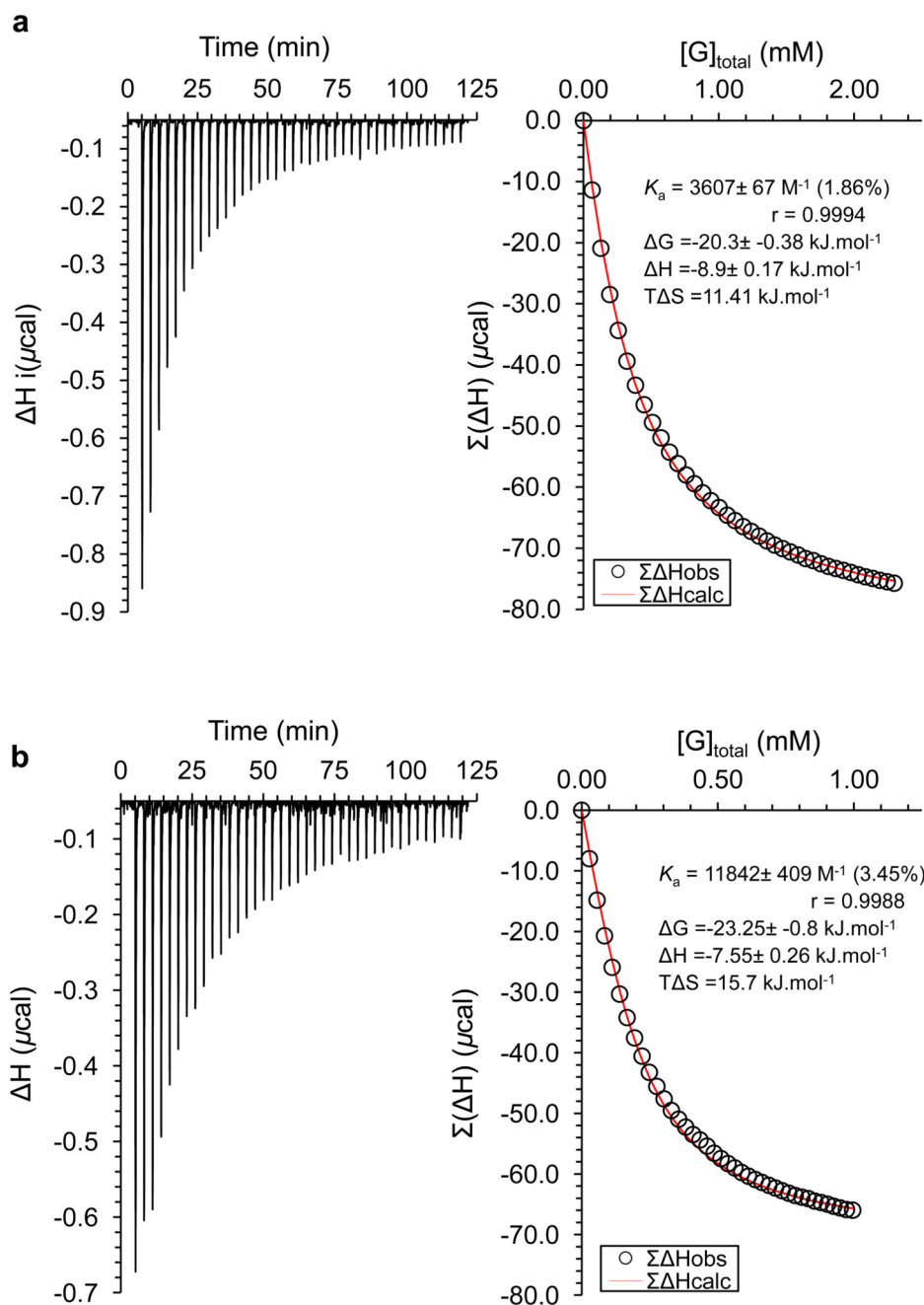
a

K_a = 3607± 67 M^{-1} (1.86%)
r = 0.9994
ΔG = -20.3± -0.38 kJ.mol^{-1}
ΔH = -8.9± 0.17 kJ.mol^{-1}
TΔS = 11.41 kJ.mol^{-1}

○ $\Sigma\Delta Hobs$
—— $\Sigma\Delta Hcalc$

b

K_a = 11842± 409 M^{-1} (3.45%)
r = 0.9988
ΔG = -23.25± -0.8 kJ.mol^{-1}
ΔH = -7.55± 0.26 kJ.mol^{-1}
TΔS = 15.7 kJ.mol^{-1}

○ $\Sigma\Delta Hobs$
—— $\Sigma\Delta Hcalc$

Fig. 3. Representative ITC data and analysis curves.
a, Addition of cellobiose **1** (n = 1) (13.05 mM) to **4** (0.2 mM, 200 μL) in water. K_a = 3600 M^{-1}. **b,** Addition of cellotetraose **1** (n = 3) (5.66 mM) to **4** (0.2 mM, 200 μL) in water. K_a = 12000 M^{-1}.
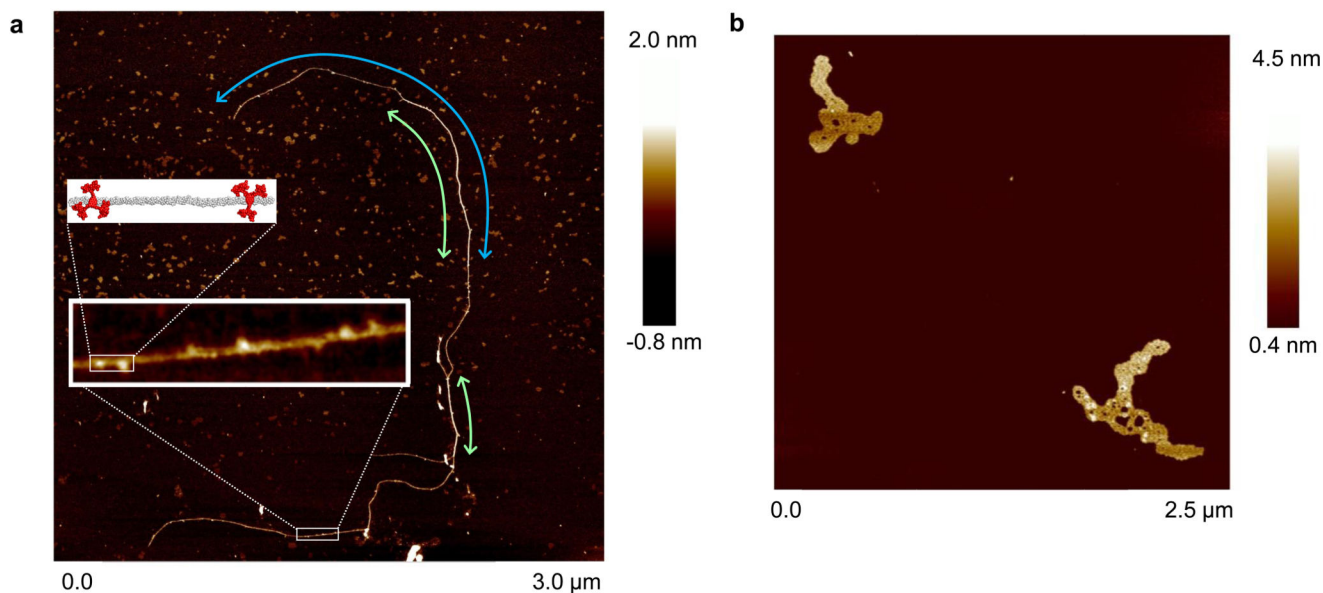
Fig. 4. AFM studies of receptor 4 + cellulose.
a, Image of cellulose (**1**) (100 nM glucosyl) + receptor **4** (1 nM) deposited from aqueous base. Green arrows show regions consistent with cellulose strand pairing, the blue arrow highlights a single cellulose molecule. Inset: A segment containing ~500 glucose monomers showing protrusions consistent with threaded receptor **4**, and a model of part of this segment containing 40 glucose units (grey) and two receptors (red). The model is energy minimized as for Fig. 2c, and accurately scaled. **b,** Control sample of cellulose, prepared as for **a** but without receptor.
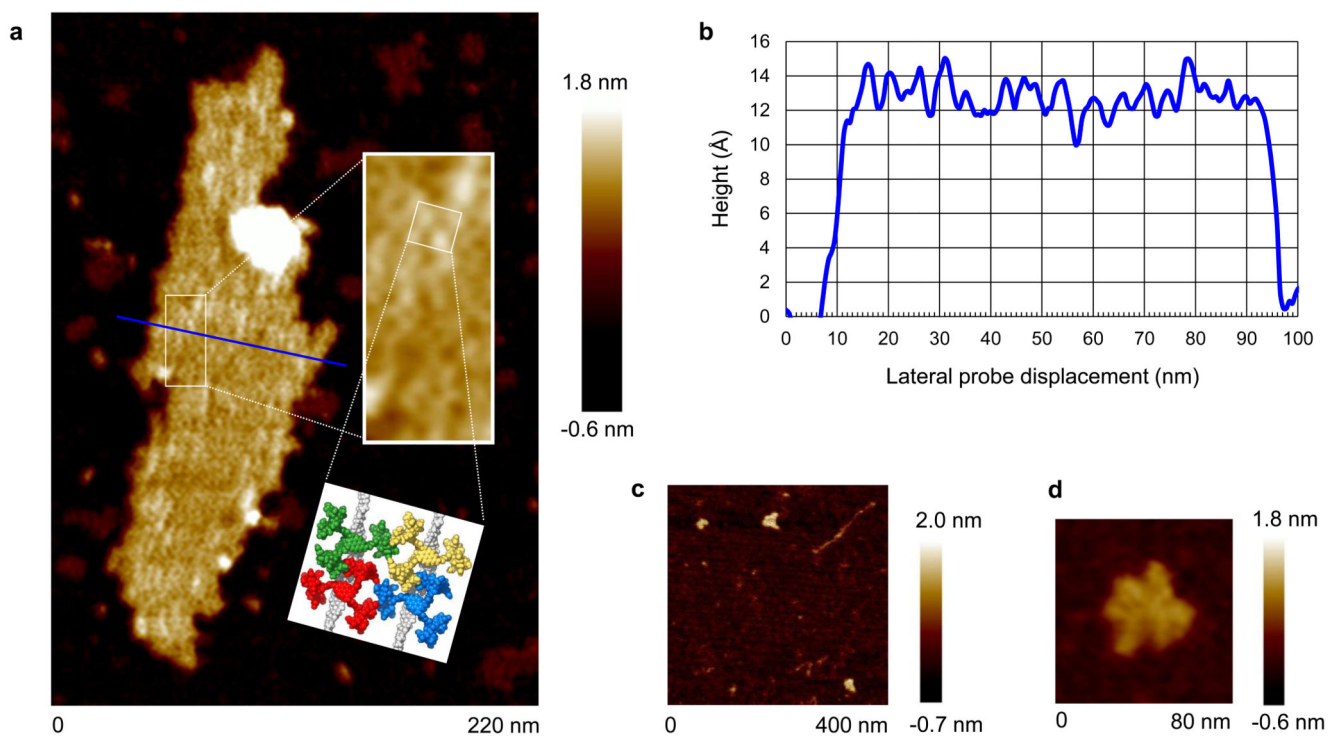
Fig. 5. AFM studies of receptor 4 + chitosan.

a, Image of chitosan **3** (n = 375-750) (1 nM glucosaminyl) + receptor **4** (0.01 nM) deposited from aqueous acid. Chitosan and receptor were mixed at pH = 1 then diluted with water by 2.5×10^7 to obtain the final concentrations. Inset: A region of the image magnified, and a modelled portion of the proposed structure constructed from two chitosan chains (grey) and four receptors (red, green, blue, yellow). The model is energy minimized as for Fig. 2c, and accurately scaled. **b,** Height profile taken across the short axis of the aggregate (blue line in part **a**). Variations are consistent with long-range order, as expected for molecular chains ~3.4 nm in width lying parallel to each other. The same periodicity was observed throughout the aggregate (see Supplementary Fig. 46). **c,** Chitosan, deposited from aqueous acid following the procedure used for **4** + chitosan. The compact objects suggest that most molecules adopt a coiled structure. A single extended strand was also observed (top right). **d,** Receptor **4**, deposited from aqueous acid following the same procedure. **d,** Receptor **4**, deposited from aqueous acid following the same procedure. Irregular aggregates are observed, up to 8 nm in height.

Table 1

Association constants (K_a) and thermodynamic parameters for receptor 4 binding carbohydrates in H_2O/D_2O at 298 K.

Carbohydrate	K_a NMR / ITC (M^{-1})	G*	H*	T S*
			(kJ.mol^{-1})	
D-Mannose (**5**)	~5 / n.d. [†]	-	-	-
D-Galactose (**6**)	18 / n.d. [†]	-	-	-
D-Glucose (**7**)	120 / n.d. [†]	-	-	-
Methyl β-D-glucoside (**8**)	240 / 260	-13.7	- 7.2	6.6
Methyl N-acetyl-β-D-glucosaminide (GlcNAc-β-OMe) (**9**)	270 / 190	-13.0	-6.4	6.7
D-Cellobiose (**1**, n = 1)	3,900[‡] / 3,600	-20.3	- 8.9	11.4
D-Cellotriose (**1**, n = 2)	5,200[‡] / 5,000	-21.1	- 8.0	13.1
D-Cellotetraose (**1**, n = 3)	n.d. [†] / 12,000	-23.3	- 7.6	15.7
D-Cellopentaose (**1**, n = 4)	n.d. [†] / 8,800	- 22.5	-8.8	13.7
D-Cellohexaose (**1**, n = 5)	n.d. [†] / 8,700	- 22.5	-8.7	13.8
N,N'-Diacetyl-D-chitobiose (**2**, n = 1)	n.d. [†] / 2,200	-19.1	-10.1	9.0
N,N',N''-Triacetyl-D-chitotriose (**2**, n = 2)	n.d. [†] / 2,400	-13.0	-6.4	6.7
D-Chitobiose (**3**, n = 1)[§]	19,000 / n.d. [†]	-	-	-

[†] Not determined.

[‡] K_a for 1:1 binding. Analysis suggests weak binding of a second substrate molecule with $K_a = 33$ M^{-1} (cellobiose) and 39 M^{-1} (cellotriose).

[§] pD=7.